

## Persistent currents in the one-dimensional mesoscopic Hubbard ring

This article has been downloaded from IOPscience. Please scroll down to see the full text article.

2008 J. Phys.: Condens. Matter 20 395209

(<http://iopscience.iop.org/0953-8984/20/39/395209>)

View [the table of contents for this issue](#), or go to the [journal homepage](#) for more

Download details:

IP Address: 129.252.86.83

The article was downloaded on 29/05/2010 at 15:11

Please note that [terms and conditions apply](#).

# Persistent currents in the one-dimensional mesoscopic Hubbard ring

Bo-Bo Wei, Shi-Jian Gu and Hai-Qing Lin

Department of Physics and the Institute of Theoretical Physics, The Chinese University of Hong Kong, Hong Kong, People's Republic of China

Received 8 May 2008, in final form 25 July 2008

Published 1 September 2008

Online at [stacks.iop.org/JPhysCM/20/395209](http://stacks.iop.org/JPhysCM/20/395209)

## Abstract

In this paper, we study persistent charge and spin currents in the ground state of the one-dimensional mesoscopic Hubbard ring with repulsive interaction based on its Bethe-ansatz solution. We find that the persistent charge current is suppressed by the on-site Coulomb interaction more significantly at half-filling than away from half-filling. As the system size increases the charge current decays exponentially as  $I \sim L^{-1}e^{-L/\xi}$  in the half-filling case and decays in a power law away from the half-filling case. We also find that the persistent spin current is suppressed by the on-site Coulomb interaction, and it decays algebraically as the system size increases both at half-filling and away from half-filling.

(Some figures in this article are in colour only in the electronic version)

## 1. Introduction

The transport properties of strongly correlated systems have attracted great theoretical and experimental attention for more than 20 years. Low-dimensional systems show some deviations from the usual Fermi liquid quasi-particle description since electron–electron correlation plays an important role in these systems [1, 2]. Byers and Yang [3] pointed out that a small metal ring pierced by a magnetic flux carries a persistent charge current, which never decays even in the presence of an impurity in the system. This phenomenon is later verified by corresponding experiments.

The persistent charge current in mesoscopic metallic and semiconducting rings pierced by a magnetic flux has been widely studied both experimentally [4–8] and theoretically [9–14]. For mesoscopic systems, the quantum coherence of electrons is very strong and the persistent current in a mesoscopic ring strongly depends on the system size. To avoid applying an uncontrolled approximation to study the quantum coherence in mesoscopic systems, people usually resort to exactly solvable models, such as the one-dimensional Heisenberg model and Hubbard model. These two models are used as effective models for the study of the transport properties in low-dimensional systems.

The one-dimensional Hubbard ring is one of the simplest models of interacting electrons on a lattice [15]. In one dimension, the model is exactly solvable by the Bethe-ansatz method [16–18]. In experiments, the one-dimensional

Hubbard model well describes optical properties of one-dimensional conductors such as TTF-TCNQ [19], various aromatic molecules, and systems of connected quantum dots [20]. It is also very interesting that the model might be helpful in analyzing the physics of the Aharonov–Bohm effect in mesoscopic metal rings [4]. Recently, several groups have studied the properties of the microscopic and mesoscopic Hubbard rings penetrating a magnetic flux, and in particular the persistent charge current in the one-dimensional Hubbard rings induced by the magnetic flux has been examined [20–25]. With the development of the spintronics, the spin degree of freedom becomes more and more important. The properties of the persistent spin current in the Hubbard ring have also been studied [22, 26].

In this paper, we study the properties of the charge and spin persistent currents in the ground state of the one-dimensional Hubbard ring pierced by a spin-dependent magnetic flux. By solving the corresponding Bethe-ansatz equations numerically, we find that the on-site Coulomb interaction always suppresses both the charge and spin persistent currents. The persistent charge current displays an exponential decay  $I_c \sim L^{-1}e^{-L/\xi}$  as the system size increases at half-filling and shows a power law away from the half-filling case, while the persistent spin current decreases algebraically as the system size increases both at half-filling and at away from half-filling, i.e.  $I_s \sim 1/L$ .

The paper is organized as follows. In section 2, we introduce the one-dimensional Hubbard model with spin-dependent Peierls phase factors and the corresponding

Bethe-ansatz solution in detail. In section 3, we study the persistent charge current and discuss the effects caused by the on-site interaction and the system size. In section 4, we study the persistent spin current for various on-site interactions and system sizes. Finally, we summarize our results in section 5.

## 2. The model and its Bethe-ansatz solution

We consider now the Hamiltonian of the one-dimensional Hubbard ring. We impose periodic boundary conditions and penetrate the system by a spin-dependent flux  $\phi_\sigma$ . The later could be represented by a spin-dependent vector potential  $A_\sigma = (hc/e)\phi_\sigma/L$ , which modifies the hopping term along the chain by the Peierls phase factor:  $t \rightarrow te^{\pm i\frac{\phi_\sigma}{L}}$  (the sign depends on the hopping direction of the electrons). Following such a procedure, the Hamiltonian reads

$$\mathcal{H} = -t \sum_{j=1}^L \sum_{\sigma=\uparrow,\downarrow} (c_{j,\sigma}^\dagger c_{j+1,\sigma} e^{-i\frac{\phi_\sigma}{L}} + \text{H.c.}) + U \sum_{j=1}^L n_{j,\uparrow} n_{j,\downarrow}. \quad (1)$$

Here the operator  $c_{j,\sigma}^\dagger$  ( $c_{j,\sigma}$ ) creates (annihilates) an electron with spin projection  $\sigma = \uparrow, \downarrow$  at site  $j$  and  $n_{j,\sigma} = c_{j,\sigma}^\dagger c_{j,\sigma}$  is the number operator at the same site.  $t$  is the hopping integral between two nearest neighboring sites;  $U > 0$  is the on-site Coulomb repulsive interaction when two electrons with different spins occupy the same site;  $L$  is the system length. Note that the energy spectrum is invariant under the replacement of  $t$  by  $-t$  [16]. We set  $t = 1$  throughout this paper.

The charge and spin current operators of the model are defined by [23, 29]

$$\mathcal{J}_\rho = \frac{ei}{L} \sum_{j=1}^L \sum_{\sigma} (c_{j,\sigma}^\dagger c_{j+1,\sigma} e^{-i\frac{\phi_\sigma}{L}} - c_{j+1,\sigma}^\dagger c_{j,\sigma} e^{i\frac{\phi_\sigma}{L}}), \quad (2)$$

and

$$\mathcal{J}_\sigma = \frac{i}{2L} \sum_{j=1}^L \sum_{\sigma} \sigma (c_{j,\sigma}^\dagger c_{j+1,\sigma} e^{-i\frac{\phi_\sigma}{L}} - c_{j+1,\sigma}^\dagger c_{j,\sigma} e^{i\frac{\phi_\sigma}{L}}), \quad (3)$$

respectively, where  $\phi_\sigma$  is in units of flux quanta  $\phi_0 = hc/e$ . The flux can be gauged out of the Hamiltonian (1), so that solving the Schrödinger equation in the presence of the magnetic flux with a periodic boundary condition is equivalent to that in the absence of the magnetic flux but with a twisted boundary condition for the wavefunctions [3], i.e.

$$\Psi(x_1, x_2, \dots, x_i + L, \dots) = e^{i\phi} \Psi(x_1, x_2, \dots, x_i, \dots). \quad (4)$$

The Hamiltonian (1) can then be solved by the nested Bethe-ansatz method, and lead to the following Lieb–Wu equations [16, 22]:

$$e^{ik_j L} = e^{i\phi_\uparrow} \prod_{\beta=1}^M \frac{\sin k_j - \Lambda_\beta + iu}{\sin k_j - \Lambda_\beta - iu}, \quad j = 1, 2, \dots, N_c \quad (5)$$

$$e^{i(\phi_\downarrow - \phi_\uparrow)} \prod_{j=1}^{N_c} \frac{\Lambda_\alpha - \sin k_j + iu}{\Lambda_\alpha - \sin k_j - iu} = - \prod_{\beta=1}^M \frac{\Lambda_\alpha - \Lambda_\beta + 2iu}{\Lambda_\alpha - \Lambda_\beta + 2iu}, \quad (6)$$

$\alpha = 1, 2, \dots, M.$

Here  $u = U/4$ ,  $N_c$  is the number of electrons and  $M$  is the number of electrons with spin down. The two sets of variables  $\{k_j\}$  and  $\{\Lambda_\alpha\}$  are the quasi-momentum and spin rapidities, respectively.

Taking the logarithm of equations (5) and (6), we arrive at the following transcendental equations [22]:

$$k_j L = 2\pi I_j + \phi_\uparrow + 2 \sum_{\beta=1}^M \tan^{-1} \left( \frac{\Lambda_\beta - \sin k_j}{U/4} \right), \quad (7)$$

$$2 \sum_{j=1}^{N_c} \tan^{-1} \left( \frac{\Lambda_\alpha - \sin k_j}{U/4} \right) = 2\pi J_\alpha + \phi_\downarrow - \phi_\uparrow + 2 \sum_{\beta=1}^M \tan^{-1} \left( \frac{\Lambda_\alpha - \Lambda_\beta}{U/2} \right). \quad (8)$$

Here  $\{I_j\}$  and  $\{J_\alpha\}$  are quantum numbers (integers or half-odd integers). All the energy eigenstates associated with the Bethe-ansatz solution are described by different occupancy configurations of the quantum numbers appearing in the coupled transcendental equations (7) and (8).  $\{I_j\}$  describes the charge degrees of freedom and  $\{J_\alpha\}$  describes the spin degrees of freedom.  $2\{I_j\}$  are even (odd) integers for even (odd)  $M$  and  $2\{J_\alpha\}$  are even (odd) for odd (even)  $N - M$ . For the ground state, the quantum number configuration is described by a continuous symmetrical sequence centered around the origin [16],

$$I_j = -\frac{N_c - 1}{2}, -\frac{N_c - 3}{2}, \dots, \frac{N_c - 1}{2}; \quad (9)$$

$$J_\alpha = -\frac{M - 1}{2}, -\frac{M - 3}{2}, \dots, \frac{M - 1}{2}. \quad (10)$$

The energy and momentum eigenvalues are given by [16]

$$E(\phi) = -2 \sum_{j=1}^{N_c} \cos k_j, \quad (11)$$

$$P = \frac{2\pi}{L} \left( \sum_{j=1}^{N_c} I_j + \sum_{\alpha=1}^M J_\alpha \right). \quad (12)$$

There are two species of particles, spin up and spin down electrons, in the system. The boundary phase angles for these two species of particles are treated as independent parameters:  $\phi_\uparrow$  and  $\phi_\downarrow$ . One can solve the transcendental equations for given  $\phi_\uparrow$  and  $\phi_\downarrow$ . To obtain the charge persistent current  $I_c$ , we let  $\phi_\uparrow = \phi_\downarrow = \phi$  and calculate the energy shift due to the magnetic flux. According to the Feynman–Hellmann theorem, the persistent charge current is given by

$$I_c = \langle \psi_0 | \mathcal{J}_\rho | \psi_0 \rangle = e \frac{\partial E_0(\phi)}{\partial \phi}. \quad (13)$$

If we take electron charge  $-e$  as the unit of the charge current, then we have

$$I_c = - \frac{\partial E_0(\phi)}{\partial \phi}. \quad (14)$$

On the other hand, setting  $\phi_\downarrow = -\phi_\uparrow = \phi$ , the energy shift gives the spin current. The persistent spin current is then given by

$$I_s = \langle \psi_0 | \mathcal{J}_\sigma | \psi_0 \rangle = - \frac{1}{2} \frac{\partial E_0(\phi)}{\partial \phi}. \quad (15)$$

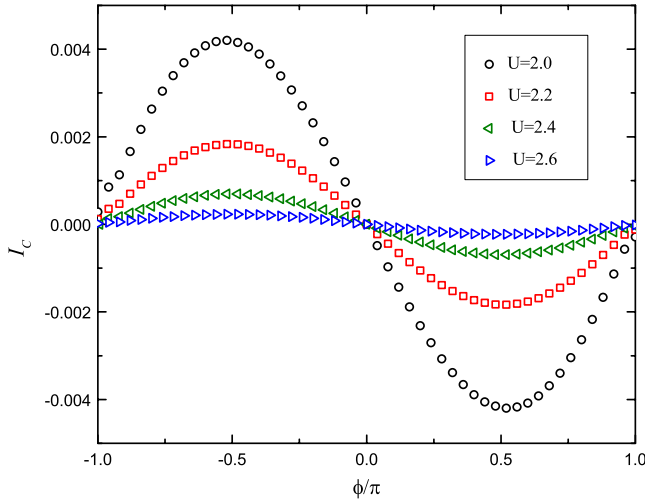


**Figure 1.** The persistent charge current  $I_c$  as a function of magnetic flux  $\phi$  for different on-site interactions with  $L = 66$  at half-filling.

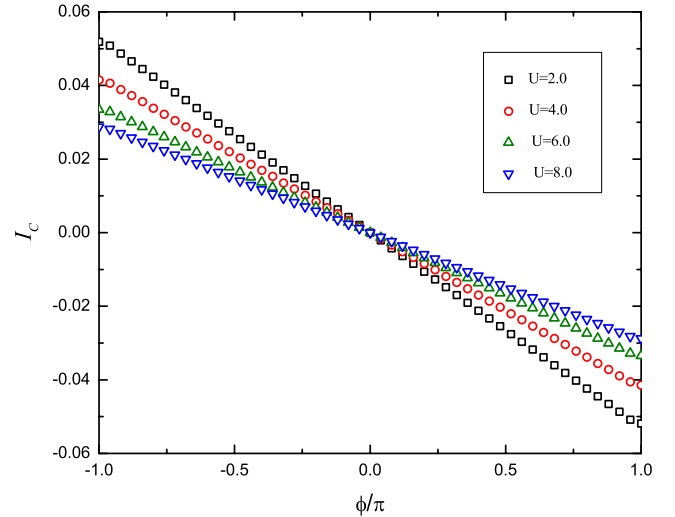


**Figure 2.** The persistent charge current as a function of magnetic flux for different on-site interactions with  $L = 66$  away from half-filling. Electron density  $\langle n \rangle = 2/5$ .

If we take electron spin  $1/2$  as the spin current unit, then we have

$$I_s = -\frac{\partial E_0(\phi)}{\partial \phi}. \quad (16)$$

### 3. The persistent charge current

As formulated by Kohn [28] and Shastry [22], the Drude weight, which is also called the charge stiffness, can be calculated as

$$D_c = \frac{L}{2} \left. \frac{\partial^2 E_0}{\partial \phi^2} \right|_{\phi=\phi_m}, \quad (17)$$

where  $\phi_m$  is the value at which the ground state energy  $E(\phi)$  is minimum. At zero temperature, a finite Drude weight is characteristic of an ideal conductor. For an insulator, whether it is a band insulator or Mott insulator, the Drude weight vanishes. At finite temperatures, the Drude weight also vanishes for normal conductors and a finite Drude weight would be a signature of superconductors.

In the large- $L$  limit and at half-filling, the flux dependence of the ground state energy of the model is [27]

$$E_0(\phi) - E_0(0) = \frac{2D_c(L)}{L}(1 - \cos \phi), \quad (18)$$

where  $D_c(L)$  is the Drude weight. The persistent charge current can be obtained as

$$I_c = -\frac{2D_c(L)}{L} \sin \phi. \quad (19)$$

Away from half-filling, the flux dependence of the ground state energy in the large- $L$  limit is [27]

$$E_0(\phi) - E_0(0) = \frac{D_c(L)}{L} \phi^2. \quad (20)$$

The persistent charge current is

$$I_c = -\frac{2D_c(L)}{L} \phi. \quad (21)$$

As is well known, the spectrum and the persistent current have a flux periodicity  $2\pi$  [3], so we consider the behavior of the current in one period from  $-\pi$  to  $\pi$ . By solving the Bethe-ansatz equations (7) and (8) numerically, we get the ground state energy as a function of flux. Taking the numerical derivative of the ground state energy with respect to flux, we can obtain the ground state persistent charge current.

#### 3.1. The persistent charge current and the on-site interaction $U$

In figures 1 and 2, the persistent charge current  $I_c$  is plotted versus the magnetic flux  $\phi$  for a 66-site system at  $\langle n \rangle = 1/2$  and  $2/5$ , respectively. Immediately we see that the behavior of the persistent charge current at half-filling is distinct from that at non-half-filling. In figure 1, we observe that the persistent charge current has sine function dependence on the magnetic flux. Moreover, with the increase of the on-site Coulomb interaction  $U$ , the magnitude of persistent charge current decreases rapidly. It nearly vanishes when  $U = 3.0$ . At the electron density  $\langle n \rangle = 2/5$  we observe that the persistent charge current scales with the magnetic flux linearly, as shown in figure 2. This property, along with the fact that the increase of the on-site Coulomb interaction  $U$  suppresses the persistent charge current slowly, is consistent with equation (20). As is well known, the half-filled Hubbard model is an insulator for  $U > 0$  since the one-electron excitation always displays an energy gap, whereas it is metallic when the filling is smaller than half. The latter could be described by the Luttinger liquid theory and one can show that the persistent current is proportional to the flux.

The behavior of the persistent charge current as a function of on-site Coulomb repulsive interaction is presented in figure 3 for various filling conditions. As shown, the persistent charge current decreases much faster at half-filling than away from half-filling with the increase of on-site Coulomb interaction and it vanishes in the large  $U$  limit at half-filling.

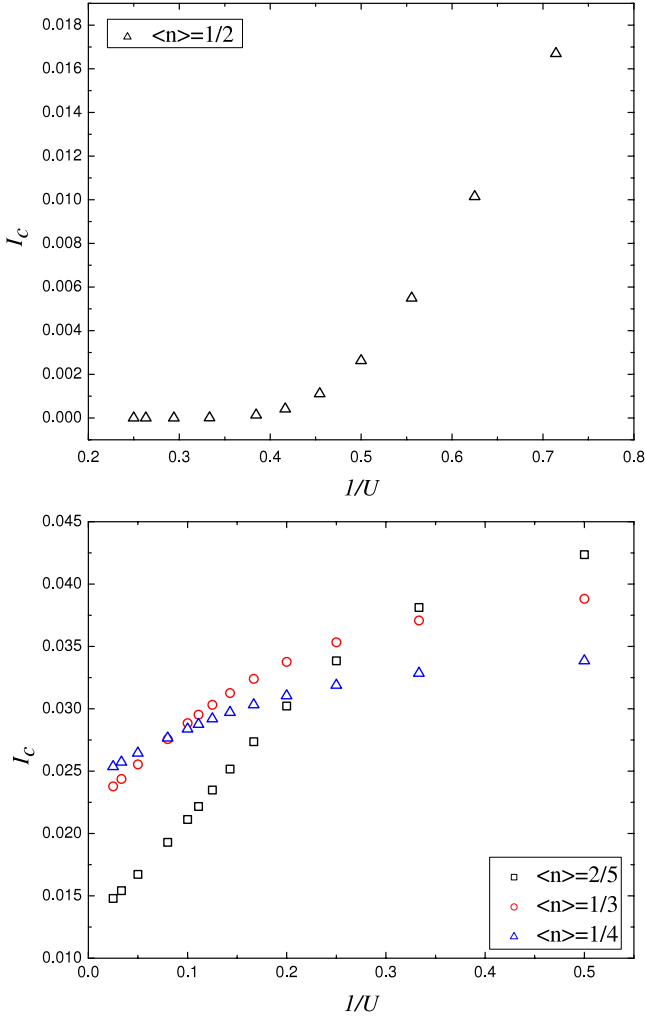


**Figure 3.** The behavior of the charge persistent current  $I_c$  as a function of the reciprocal of on-site Coulomb interaction  $1/U$  at  $L = 66$  for different electron densities when  $\phi = -0.8\pi$ .

However, if the filling is smaller than half, the persistent charge current decreases slowly with the increase of on-site Coulomb interaction, and does not tend to zero even if  $U$  is very large. The reason is that the model is metallic away from half-filling. To examine the effect of the on-site Coulomb interaction on the persistent charge current quantitatively, we show in figure 4 the persistent current for electron density  $\langle n \rangle = 1/2$ , from which we extract the dependence of the persistent charge current  $I_c$  on  $U$ . We find that at half-filling the charge current varies as  $I \sim e^{-U^2/\xi}$  with  $\xi \simeq 1$ . The parameter  $\xi$  is carefully adjusted to get a best fit of the data in figure 4.

### 3.2. The persistent charge current and the system size $L$

In mesoscopic systems, the persistent current is greatly dependent on the system size. The size dependence of the mesoscopic ring can be used to determine different phases, such as metal or insulator [29]. A perfect metal will be characterized by the persistent charge current scaling as  $1/L$ , while for an insulator the charge persistent current decays exponentially, i.e.  $I_c \sim L^{-1}e^{-L/\xi}$ , where  $\xi$  is the localization length.

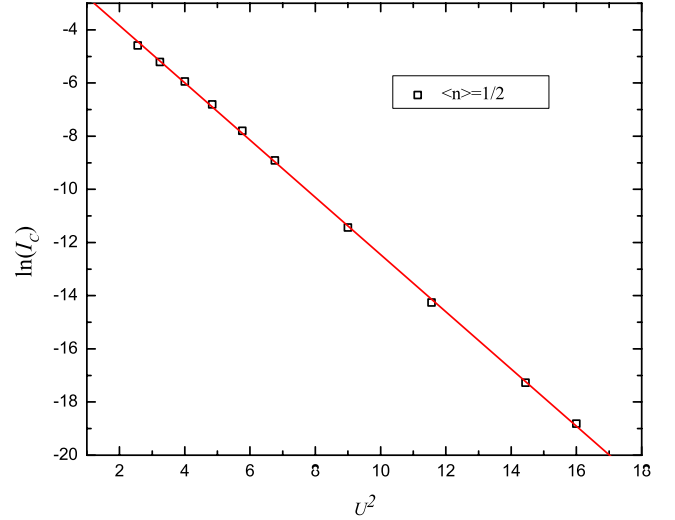


**Figure 4.** Logarithm of the charge persistent current  $\ln(I_c)$  versus  $U^2$  at half-filling with system size  $L = 66$  when  $\phi = -0.8\pi$ .

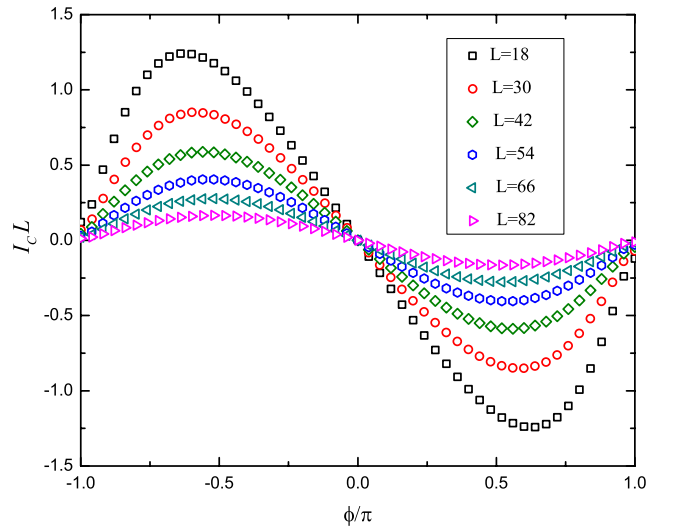


**Figure 5.** The persistent charge current  $I_c$  versus magnetic flux  $\phi$  at half-filling for several system sizes  $L$ , respectively, when the on-site Coulomb interaction  $U = 2.0$ .

Firstly, we examine the size dependence for the free fermions of the model ( $U = 0$ ). The ground state energy of the model when  $U = 0$  is

$$E(\phi) = -2 \frac{\cos(\phi/L)}{\sin(\pi/L)}. \quad (22)$$

We take  $L = 4k + 2$  to avoid energy degeneracy. Then the charge persistent current for the free fermions of the model is given by

$$I_c(\phi) = \frac{2 \sin(\phi/L)}{L \sin(\pi/L)}. \quad (23)$$

So we can find that the size dependence of the persistent charge current for the free fermion model scales as  $1/L$  in large  $L$ . This fact verifies that the system is metallic at  $U = 0$ .

Figures 5 and 6 show the behavior of the persistent charge current of the system as a function of the magnetic

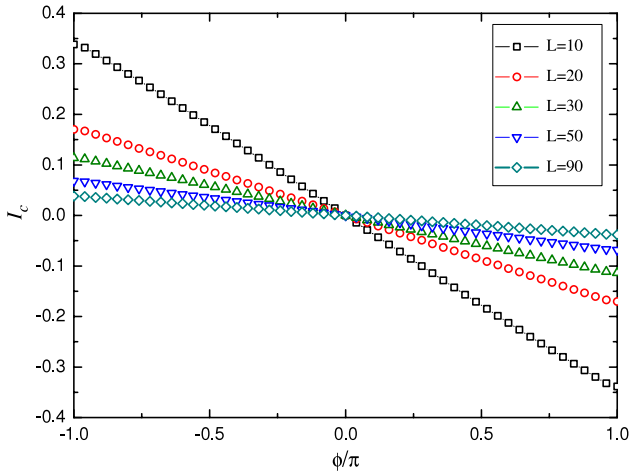


**Figure 6.** The persistent charge current  $I_c$  versus magnetic flux  $\phi$  away from half-filling for several system sizes  $L$ , respectively, when the on-site Coulomb interaction  $U = 2.0$ . Electron density  $\langle n \rangle = 2/5$ .

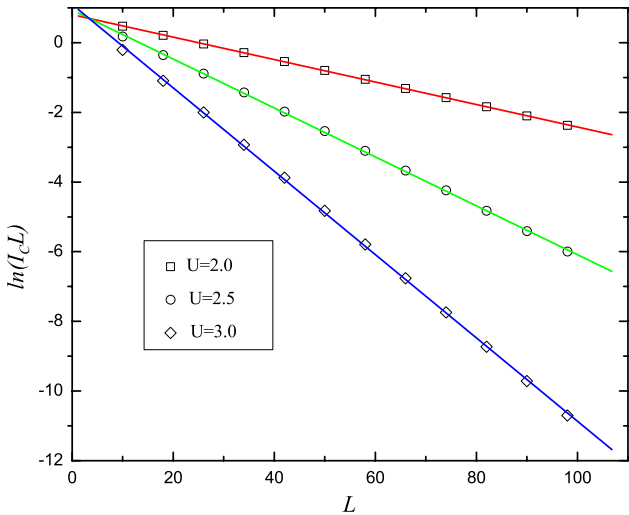


**Figure 7.** Logarithm of the charge persistent current  $\ln(I_c L)$  as a function of the number of sites  $L$  at half-filling, where  $\phi = 0.6\pi$ , for on-site interaction  $U = 2.0, 2.5$  and  $3.0$  respectively. The lines represent  $I \sim L^{-1}e^{-L/\xi}$ , with  $\xi$  dependent on  $U$ .

flux threading the ring at half-filling and away from half-filling respectively for several system sizes. We find that the charge current has a sine function form with the magnetic flux threaded at half-filling, while it is a linear function away from half-filling. With the increase of system sizes, the magnitude of the charge persistent current decreases monotonically both at half-filling and away from half-filling. To examine the conducting behavior of the system at different filling conditions, we present the persistent charge current as a function of the system sizes for different values of on-site Coulomb interaction, for the half-filling case in figure 7 and away from the half-filling case in figure 8, from which we can extract the dependence of the charge current  $I_c$  on the size of the system. We observe, from figure 7, that the persistent charge current varies as  $I_c \sim L^{-1}e^{-L/\xi}$ , with  $\xi \simeq 31.0, 14.2$  and  $8.4$  for  $U = 2.0, 2.5$  and  $3.0$ , respectively at half-filling.

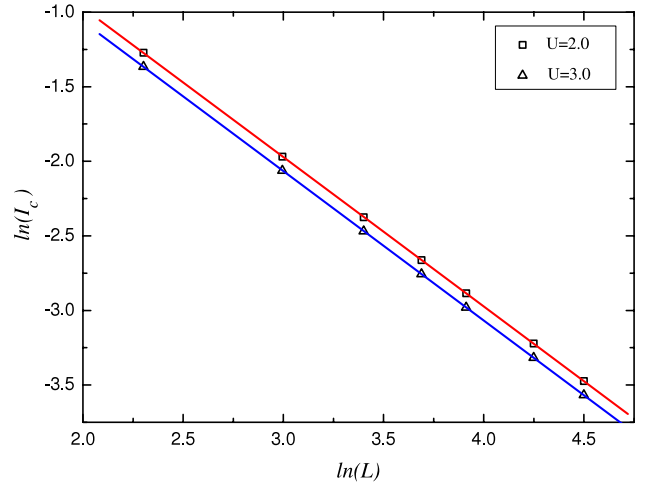


**Figure 8.** Logarithm of the charge persistent current  $\ln(I_c)$  as a function of the number of sites  $\ln(L)$  away from half-filling, where  $\phi = -0.8\pi$ , for on-site interaction  $U = 2.0$  and  $3.0$  respectively. Electron density  $\langle n \rangle = 2/5$ . The lines represent  $I \sim L^{-1+\delta}$ , where  $\delta$  is a small number.

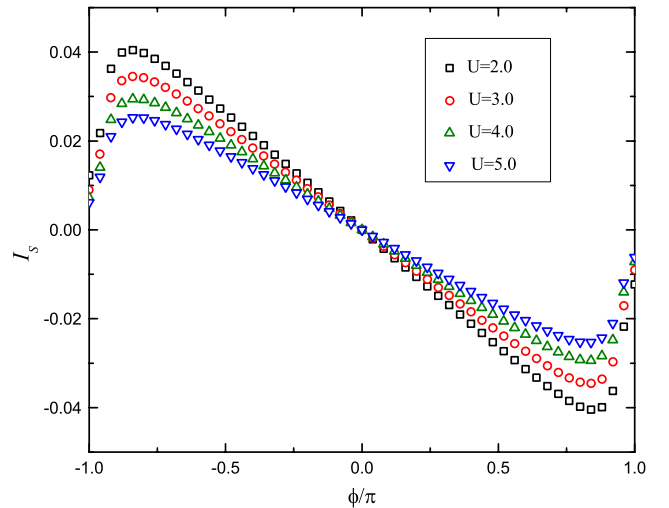


**Figure 9.** The persistent spin current  $I_s$  versus magnetic flux  $\phi$  at  $L = 66$  for different on-site Coulomb interactions  $U$  at half-filling.

The localization length can be given by the slope of the straight line in figure 7, which is obtained by performing the best fit of the data in the figure 7 on a plot of  $\ln(I_c L)$  versus the size number  $L$ . Meanwhile, one can see that the localization length decreases with the increase of the on-site Coulomb repulsive interaction. Away from the half-filling case, we can see, from figure 8, that the charge current decreases with the system sizes in a power law behavior,  $I_c \sim L^{-1+\delta}$ ,  $\delta = -0.001, -0.002$  for  $U = 2.0, 3.0$ , respectively, which verifies the Hubbard ring is a charge conductor away from half-filling.

## 4. The persistent spin current

### 4.1. The persistent spin current and the on-site interaction $U$

Figures 9 and 10 show the persistent spin current  $I_s$  versus the magnetic flux  $\phi$  for various on-site coulomb interactions

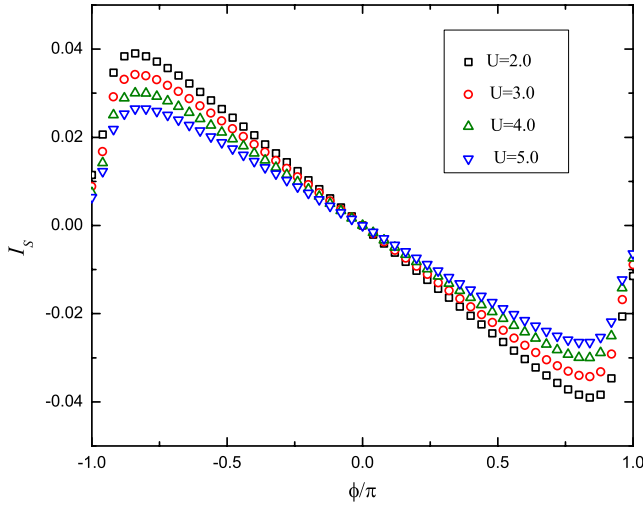


**Figure 10.** The persistent spin current  $I_s$  versus magnetic flux  $\phi$  at  $L = 66$  for different on-site Coulomb interactions  $U$  away from half-filling. Electron density  $\langle n \rangle = 2/5$ .

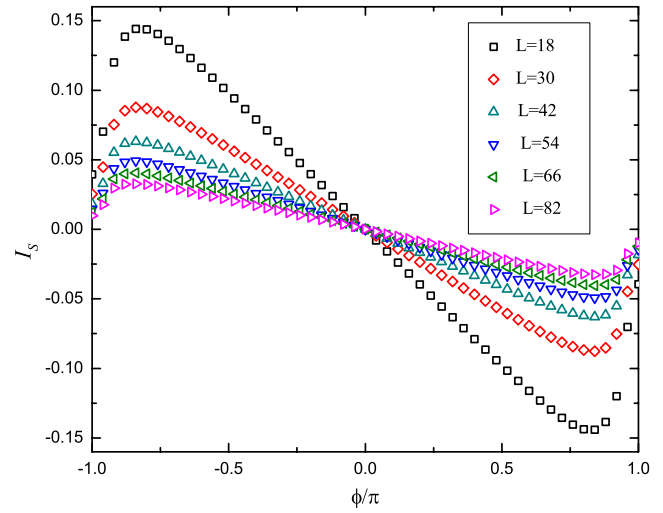


**Figure 12.** The persistent spin current  $I_s$  versus the magnetic flux  $\phi$  at half-filling for several system sizes when on-site Coulomb interaction  $U = 2.0$ .

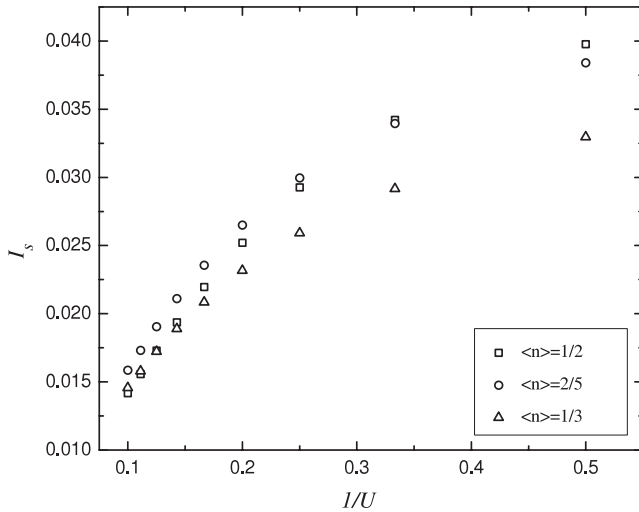


**Figure 11.** The persistent spin current  $I_s$  versus the reciprocal of the on-site Coulomb interaction  $1/U$  at  $L = 66$  for the electron density  $\langle n \rangle = 1/2, 2/5$  and  $1/3$  respectively when  $\phi = -0.8\pi$ .

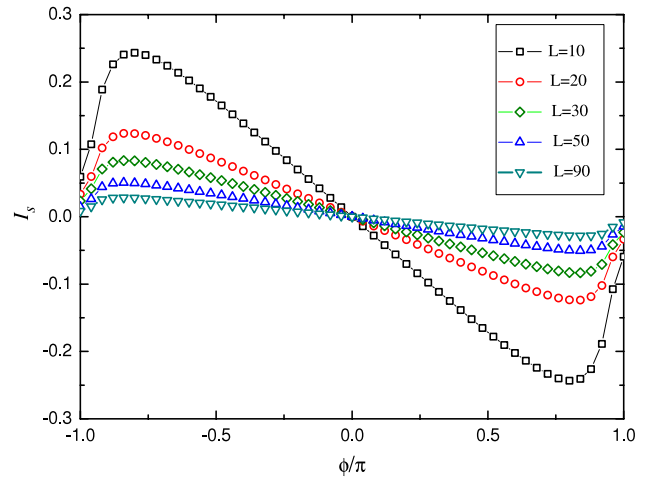


**Figure 13.** The persistent spin current  $I_s$  versus the magnetic flux  $\phi$  away from half-filling for several system sizes when on-site Coulomb interaction  $U = 2.0$ .

$U$ , and for the electron density  $\langle n \rangle = 1/2$  and  $\langle n \rangle = 2/5$  respectively. We see that the behavior of the spin current is different from that of the charge current both at half-filling and away from half-filling, which is neither a sine dependence on the magnetic flux nor a linear function of magnetic flux. We observe that the on-site Coulomb interaction also suppresses the persistent spin current both at half-filling and away from half-filling. Moreover, we can see that the spin current is insensitive to the electron density of the model. This phenomenon is obviously different from the behavior of the charge current.

To study the effect of on-site Coulomb interaction on the persistent spin current, we present the spin current of the model as a function of the on-site Coulomb interaction at electron density  $\langle n \rangle = 1/2, 2/5$  and  $1/3$  respectively in figure 11. We observe that with the increase of the on-site Coulomb

interaction  $U$  the persistent spin current always decreases, both at half-filling and away from half-filling. Moreover, the persistent spin current tends to respond more sensitively at higher filling when  $U$  increases. Meanwhile, we find that the persistent spin current does not tend to zero even when  $U$  is very large, which is true both at half-filling and away from half-filling. This is because the model effectively becomes a Heisenberg model when  $U$  tends to infinity. The persistent spin current exists in the Heisenberg model, which has been studied by many people [30, 31].

#### 4.2. The persistent spin current and the system size $L$

We present the persistent spin current of the system as a function of the magnetic flux for several sites when  $U = 2.0$  for half-filling and away from half-filling in figures 12 and 13, respectively. We find that, with the increase of the number

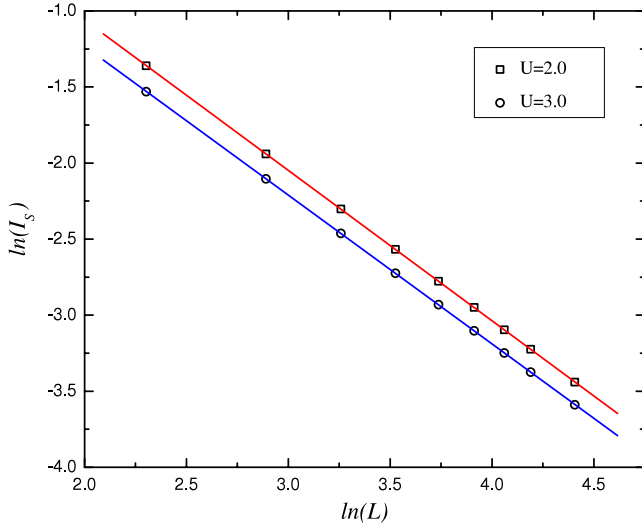


**Figure 14.** Logarithm of  $I_s$  versus  $L$  at half-filling for  $U = 2.0$  and  $3.0$  respectively when  $\phi = -0.8\pi$ . The lines represent  $I_s \sim L^{-1+\delta}$ , where  $\delta$  is a small number.

of sites, the persistent spin current decreases gradually both at half-filling and away from half-filling.

To examine the spin conducting properties of the system, we do finite size scaling of the spin current. Figures 14 and 15 present the persistent spin current of the model as a function of the system sizes for half-filling and away from half-filling respectively. The spin current decreases with the system size as  $L^{-1+\delta}$  at half-filling, with  $\delta = 0.01$  and  $0.02$  for  $U = 2.0$  and  $3.0$  respectively. The exponent  $\delta$  is obtained as the slope of the straight fitting line in figure 14. The spin current decays with the system sizes as  $L^{-1+\delta}$  away from half-filling, with  $\delta = 0.02$  and  $0.03$ . The exponent  $\delta$  is obtained from the best fit of the data in figure 15.

## 5. Summary

We have studied the behavior of the persistent charge current and persistent spin current on a mesoscopic ring pierced by a spin-dependent magnetic flux. By solving the Bethe-ansatz equations of the one-dimensional Hubbard model numerically, we calculated the persistent charge current and persistent spin current of the ground state as a function of the magnetic flux. Then we study the effect of both the on-site Coulomb repulsive interaction and the system size on the persistent currents. The behavior of the charge persistent current at half-filling is quite different from that away from half-filling. The persistent charge current has sine function form with respect to the magnetic flux at half-filling, while it is a linear function away from half-filling. We also find that the persistent charge current shows a dominant exponential decay,  $I \sim L^{-1}e^{-L/\xi}$ , in the half-filling case with the number of sites of the system while it shows a power law decay,  $L^{-1+\delta}$ , away from half-filling. The persistent spin current also decreases with the increase of the on-site Coulomb interaction. The behavior of the persistent spin current is insensitive to the electron density of the system, and it decays as  $L^{-1+\delta}$  with the system size both at half-filling and away from half-filling.

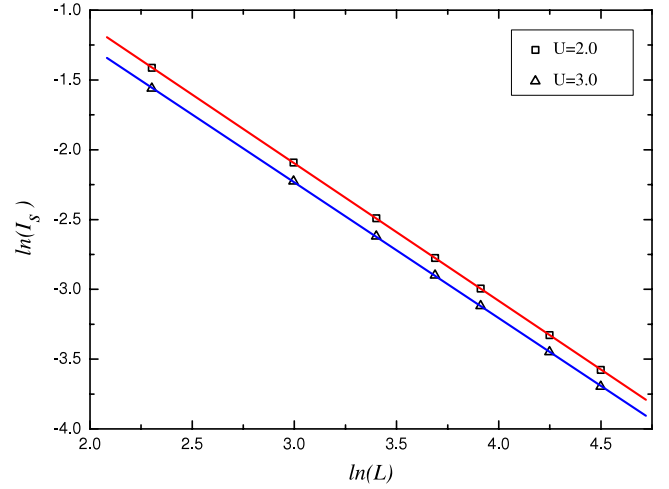


**Figure 15.** Logarithm of  $I_s$  versus  $L$  away from half-filling for  $U = 2.0$  and  $3.0$  respectively when  $\phi = -0.8\pi$ . The lines represent  $I_s \sim L^{-1+\delta}$ , where  $\delta$  is a small number.

## Acknowledgments

We thank Mr W L Chan for critically reading our paper. This work is supported by RGC Grant CUHK 402107.

## References

- [1] Dressel M, Schwartz A, Grüner G and Degiorgi L 1996 *Phys. Rev. Lett.* **77** 398
- [2] Kobayashi K, Mizokawa T, Fujimori A, Isobe M and Ueda Y 1998 *Phys. Rev. Lett.* **80** 3121
- [3] Byers N and Yang C N 1961 *Phys. Rev. Lett.* **7** 46
- [4] Levy L P, Dolan G, Dunsmuir J and Bouchiat H 1990 *Phys. Rev. Lett.* **64** 2074
- [5] Chandrasekhar V, Webb R A, Brady M J, Ketchen M B, Gallagher W J and Kleinsasser A 1991 *Phys. Rev. Lett.* **67** 3578
- [6] Mailly D, Chapelier C and Benoit A 1993 *Phys. Rev. Lett.* **70** 2020
- [7] Reulet B, Ramin M, Bouchiat H and Mailly D 1995 *Phys. Rev. Lett.* **75** 124
- [8] Jariwala E M Q, Mohanty P, Ketchen M B and Webb R A 2001 *Phys. Rev. Lett.* **86** 1594
- [9] Landauer R and Büttiker M 1985 *Phys. Rev. Lett.* **54** 2049
- [10] Cheung H F, Gefen Y, Riedel E K and Shih W H 1988 *Phys. Rev. B* **37** 6050
- [11] Altshuler B L, Gefen Y and Imry Y 1991 *Phys. Rev. Lett.* **66** 88
- [12] von Oppen F and Riedel E K 1991 *Phys. Rev. Lett.* **66** 84
- [13] Schmid A 1991 *Phys. Rev. Lett.* **66** 80
- [14] Abraham M and Berkovits R 1993 *Phys. Rev. Lett.* **70** 1509
- [15] For example, Montorsi A (ed) 1992 *The Hubbard Model—a Reprint Volume* (Singapore: World Scientific)
- [16] Lieb E and Wu F Y 1968 *Phys. Rev. Lett.* **20** 1445
- [17] Essler F H L, Frahm H, Göhmann F, Klümper A and Korepin V E 2005 *The One-Dimensional Hubbard Model* (Cambridge: Cambridge University Press)
- [18] Li Y Q and Gruber C 1998 *Phys. Rev. Lett.* **80** 1034
- [19] Maldague P F 1977 *Phys. Rev. B* **16** 2437
- [20] Kusmartsev F V 1991 *J. Phys.: Condens. Matter* **3** 3199
- [21] Yu N C and Fowler M 1992 *Phys. Rev. B* **45** 11795
- [22] Shastry B S and Sutherland B 1990 *Phys. Rev. Lett.* **65** 243
- [23] Peres N M R, Sacramento P D and Carmelo J M P 2001 *J. Phys.: Condens. Matter* **13** 5135



- [24] Carmelo J M P, Gu S J and Peres N M R 2007 *Europhys. Lett.* **78** 17005
- [25] Gu S J, Peres N M R and Carmelo J M P 2007 *J. Phys.: Condens. Matter* **19** 506203
- [26] Shiba H 1972 *Phys. Rev. B* **6** 930
- [27] Stafford C A and Millis A J 1993 *Phys. Rev. B* **48** 1409
- [28] Kohn W 1964 *Phys. Rev. A* **133** 171
- [29] Bouzerar G, Poilblanc D and Montambaux G 1994 *Phys. Rev. B* **49** 8258
- [30] Dias F C, Pimentel I R and Henkel M 2006 *Phys. Rev. B* **73** 075109
- [31] Hu Z X and Li Y Q 2007 *Mod. Phys. Lett. B* **21** 327